

# Multivalent Nanofibers of a Controlled Length: Regulation of Bacterial Cell Agglutination

Dong-Woo Lee,<sup>†</sup> Taehoon Kim,<sup>†</sup> Il-Soo Park, Zhegang Huang, and Myongsoo Lee\*<sup>‡</sup>

Center for Bio-Responsive Assembly and Department of Chemistry, Seoul National University, 1 Gwanak-ro, Gwanak-gu, Seoul 151-747, Korea

**S** Supporting Information

**ABSTRACT:** Control of the size and shape of molecular assemblies on the nanometer scale in aqueous solutions is very important for the regulation of biological functions. Among the well-defined supramolecular structures of organic amphiphiles, one-dimensional nanofibers have attracted much attention because of their potential applications in biocompatible materials. Although much progress has been made in the field of self-assembled nanofibers, the ability to control the fiber length remains limited. The approach for control of the fiber length presented herein overcomes this limitation through the coassembly of amphiphilic rod-coil molecules in which the crystallinity of the aromatic segment can be regulated by  $\pi$ - $\pi$  stacking interactions. The introduction of carbohydrate segments into the fiber exterior endows the nanofibers with the ability to adhere to bacterial cells. Notably, the fiber length systematically regulates the agglutination and proliferation of bacterial cells exposed to these fibers.

One of the fascinating features of carbohydrate-coated nanofibers is their multivalent interactions with specific biomolecules. A recent series of studies revealed that the carbohydrate-coated one-dimensional nanostructures formed through the self-assembly of small carbohydrate-containing molecules, such as discotic compounds<sup>1</sup> and peptide amphiphiles,<sup>2-6</sup> specifically bind to multiple mannose-binding proteins. These fibrillar structures coated by carbohydrates are excellent multivalent ligands for specific receptors on cell surfaces<sup>7,8</sup> and can modulate carbohydrate-receptor binding events associated with biological processes.<sup>9,10</sup> Although much progress has been made in the field of carbohydrate nanofibers, the ability to control the length of carbohydrate-coated nanofibers remains limited. To date, only a few methods have been reported to control fiber length in self-assembled systems, irrespective of the biological functions of these systems. The research group of Manners and Winnik reported that the length of monodisperse cylindrical micelles could be well-controlled in organic solvent by crystallization-driven living self-assembly of block copolymers.<sup>11-13</sup> Besenius et al. reported another approach, charge repulsion, to control the length of nanofibers in water.<sup>14</sup> Another example is the template approach, in which dumbbell-shaped rod amphiphiles are used as templates for peptide assembly on their surfaces to form nanofibers with a controlled length.<sup>15</sup> We previously reported that a rigid-

flexible combination in an amphiphilic system leads to the formation of nanofibers with a well-defined width in aqueous solutions. These nanofibers are based on an amorphous aromatic core that undergoes a sol-gel interconversion in response to external stimuli.<sup>16-18</sup> We hypothesized that varying the crystallinity of the aromatic cores in nanofibers would regulate the fiber length by controlling the  $\pi$ - $\pi$  stacking interactions. With this idea in mind, we performed coassembly experiments to regulate the crystallinity of the aromatic cores of carbohydrate nanofibers for the purpose of controlling the fiber length, which might in turn control the biological functions of bacterial cells by altering the multivalent interactions.

In this communication, we report the ability to control the length of carbohydrate-coated nanofibers through the coassembly of carbohydrate rod amphiphile **1**, which has a highly crystalline aromatic core, with **2**, which has a less crystalline aromatic core than **1**. With increasing content of **2**, the fiber length decreases from a few micrometers to a few tens of nanometers as the result of the decreasing crystallinity of the aromatic cores. These nanofibers bind bacterial cells through multivalent carbohydrate-receptor interactions and systematically regulate the proliferation of the bacterial cells, with the effect depending on the fiber length. The amphiphiles that form these nanofibers consist of aromatic segments that are laterally grafted by hydrophilic mannose moieties (Figure 1). These amphiphilic molecules were synthesized in a stepwise fashion according to the procedure described in the Supporting Information (SI). The resulting aromatic amphiphiles were characterized by NMR spectroscopy and MALDI-TOF mass

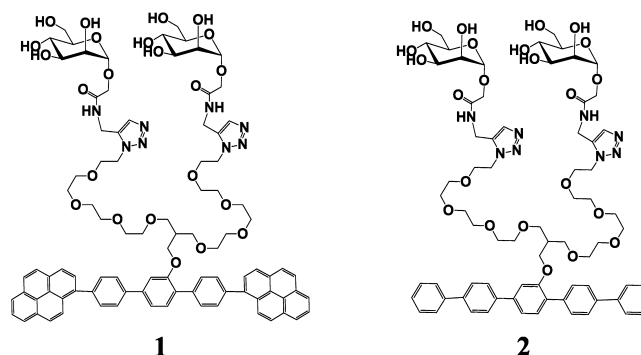


Figure 1. Chemical structures of amphiphiles **1** and **2**.

Received: July 12, 2012

Published: August 24, 2012

spectrometry, and the results were in full agreement with the structures presented herein.

The formation of self-assembled nanostructures was initially investigated by transmission electron microscopy (TEM). In addition, cryogenic TEM (cryo-TEM) was also undertaken to investigate the self-assembled structures in bulk solutions (Figure S2 in the SI). Figure 2 shows micrographs obtained for

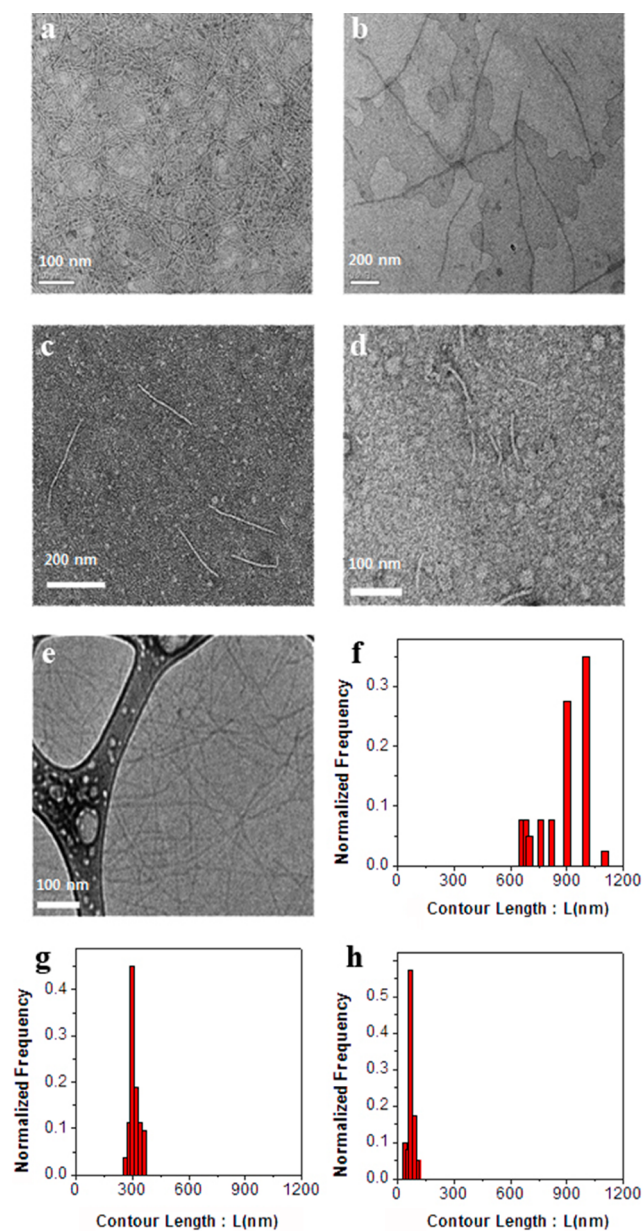


**Figure 2.** (a–d) TEM images of (a) **1** in water ( $60 \mu\text{M}$ ) and (b–d) coassembled samples with decreasing nanofiber length and increasing proportion of **2**: (b) 1:2 = 85:15; (c) 1:2 = 50:50; (d) **2**. (e) Cryo-TEM image of **1**. (f–h) Contour length distributions of samples (b–d), respectively.

$60 \mu\text{M}$  aqueous solutions of **1**, **2**, and coassembled amphiphiles cast onto TEM grids. The TEM image of **1**, which is based on pyrene units and was negatively stained with uranyl acetate, clearly shows long, rigid nanofibers with a uniform width of  $\sim 6$  nm and lengths of  $> 2 \mu\text{m}$ . We could not accurately measure the lengths of the nanofibers because the fibers extended beyond the boundary of the TEM image. In contrast, **2**, which is based

on a pentaphenylene rod, self-assembles into short fibers with an average length of 70 nm. The combination of these two nanofibers through coassembly might result in the formation of nanofibers with different lengths. To test this hypothesis, we performed coassembly experiments with **1** and **2**. Interestingly, the length of the nanofibers systematically decreased from a few micrometers to less than 70 nm as the amount of **2** increased. When the length distribution of the nanofibers based on measurements of  $> 150$  fibers in the images was evaluated, the average lengths of the nanofibers were 1  $\mu\text{m}$ , 300 nm, and 70 nm for 1:2 mole ratios of 85:15, 50:50, and 0:100, respectively.

To gain insight into the packing arrangements of the rod segments in nanofibers of different lengths, we used UV–vis (Figure S3) and fluorescence spectroscopy (Figure 3a). When

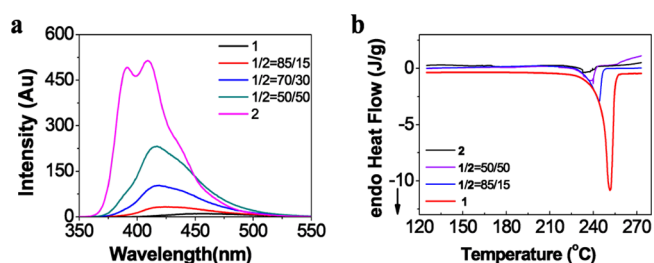


**Figure 3.** (a) Fluorescence spectra of amphiphiles ( $60 \mu\text{M}$ ) upon excitation at 316 nm. (b) DSC traces for **1**, **2**, and coassembled amphiphiles upon heating.

the coassembled samples were excited at the absorption maximum of **2**, the emission peak of **2** was gradually red-shifted and quenched with increasing **1** content, which suggested that the energy transfer process between two amphiphiles occurred more efficiently, indicating that there are increasing  $\pi$ – $\pi$  stacking interactions. To assess further the packing arrangements of the aromatic cores of **1**, **2**, and the coassembled amphiphiles, the thermal behavior of the freeze-dried samples was evaluated by differential scanning calorimetry (DSC). The melting transition temperatures ( $T_m$ ) and the corresponding enthalpy changes of all of the samples obtained from the DSC heating scans (Figure 3b) are summarized in Table S1 in the SI. As shown in Figure 3b and Table S1, an increase in the relative amount of **2** led to a shift in the melting peak to lower temperatures along with a significant decrease in the heat of fusion, demonstrating that the crystallinity of the aromatic core of **1** is disrupted by the addition of **2**. These results suggest that the packing arrangements within the aromatic core play a critical role in controlling the length of the self-assembled nanofibers. Indeed, the high crystallinity of the aromatic core of **1**, as reflected by the large heat of fusion, leads to the formation of long nanofibers with a micrometer-scale length. In contrast, amorphous aromatic cores with very low heats of fusion, as in the case of **2**, give rise to short fibers with lengths of only a few tens of nanometers. The systematic replacement of pyrene units with phenyl units through coassembly would result in the disruption of the packing of the aromatic segments, thereby reducing the assembly forces of the molecules. Consequently, the fiber length of **1** systematically decreased with the successive addition of **2**.

To gain further insight into the variation in the length of the fibers, we measured the solution viscosity and performed static light scattering (SLS) experiments. The solution viscosities of **1**, **2**, and the coassembled amphiphiles were measured at  $27 \text{ }^\circ\text{C}$  using a capillary viscometer. The results showed that the

viscosity dramatically increases with an increase in the relative amount of **1** (Figure 4a). This result could be attributed to an

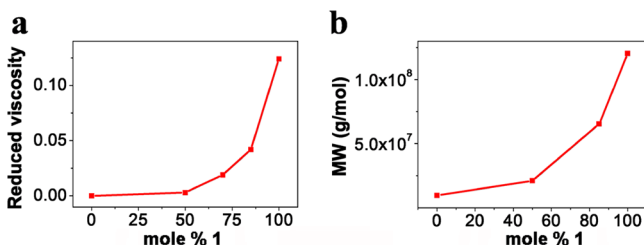


**Figure 4.** (a) Reduced viscosity and (b) absolute molecular weight (from SLS) as functions of the content of **1** (in mol %).

increase in the fiber length. This hypothesis was confirmed by molecular weight measurements with SLS. Analysis of the molecular weight using a Zimm plot showed a dramatic decrease from  $1.2 \times 10^8$  g/mol for **1** to  $9.6 \times 10^6$  g/mol for **2**, and this trend is consistent with the viscosity results (Figure 4b). These results, together with the TEM data, demonstrate that the nanofiber length can be controlled by varying the 1:2 mole ratio.

The simultaneous presentation of mannose epitopes on a nanofiber scaffold creates a multivalent ligand that has a high affinity for carbohydrate receptors.<sup>19</sup> For this reason, multivalent carbohydrate-coated molecules and nanofibers have been utilized as competitive inhibitors targeting several biological interactions.<sup>20</sup> Recent reports have shown that multivalent carbohydrate-coated nanofibers can induce agglutination and inhibit the motility of pathogenic cells.<sup>21–23</sup> To investigate the multivalent interactions between nanofibers and *Escherichia coli* cells, we choose an *E. coli* strain expressing the mannose-binding adhesion protein FimH in its type-1 pili (ORN 178-GFP). As shown in Figure 5, when the *E. coli* were incubated with pure **1** and with coassembled samples, clusters of fluorescent bacteria of different sizes were observed. The cluster size decreased with decreasing fiber length, indicating that the length of the mannose nanofibers plays a critical role in the agglutination of bacterial cells. In contrast, we did not observe bacterial agglutination with **2**, most likely because of the low aggregation stability of the fibers. To examine the ability of the nanofibers to agglutinate bacterial cells, agglutination index (AI) assays were performed (Figure 6a). Significant differences among the samples were observed in terms of the ability to agglutinate *E. coli*. The evaluated AI systematically increased with increasing **1** content. These results demonstrate that the length of the nanofibers has a significant influence on the formation of bacterial clusters and is a critical factor controlling agglutination. This result suggests that long nanofibers are able to aggregate *E. coli* cells dispersed in media, forming large bacterial clusters. However, the ability to aggregate *E. coli* decreases with decreasing fiber length (Scheme 1).

Given adequate nutrition conditions and a pleasant environment, single-cell organisms such as *E. coli* can survive by proliferating, but uncontrolled bacterial proliferation is closely related to abnormal responses such as inflammation and autoimmune diseases. Therefore, the controlled proliferation of bacterial cells has emerged as an important issue. As previously reported,<sup>2,3,7,8</sup> there is a close relationship between the form of bacterial clusters and the repression of the proliferation activity of bacteria cells. On the basis of these results, we anticipated

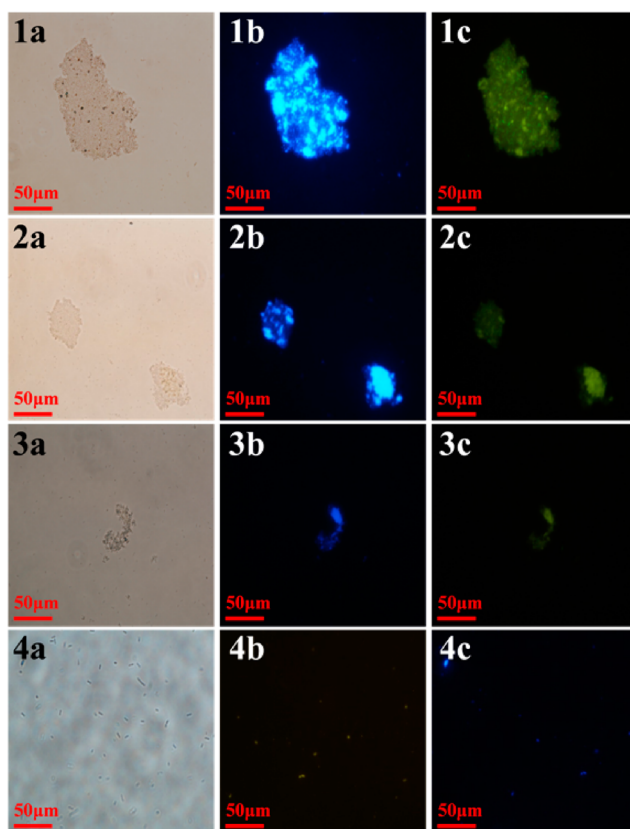


**Figure 5.** Microscopy images from fluorescence colocalization studies of *E. coli* (yellow) with nanofibers (blue): (a) bright-field, (b) fluorescence (excitation filter at  $\lambda_{\text{ex}} = 450\text{--}490$  nm), and (c) fluorescence (excitation filter at  $\lambda_{\text{ex}} = 340\text{--}380$  nm) images for incubation with (1) **1**, (2) 1:2 = 85:15, (3) 1:2 = 50:50, and (4) **2**.

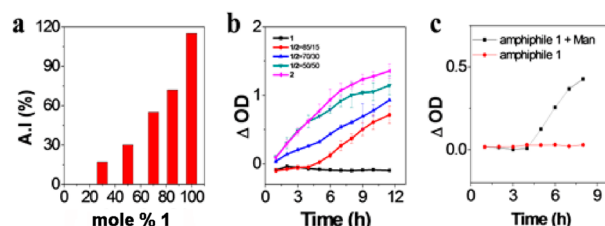
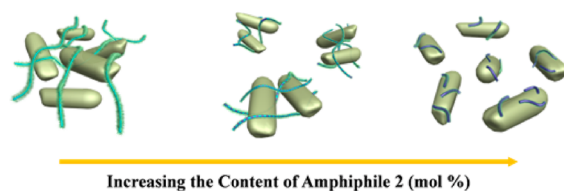


**Figure 6.** (a) Effect of the length of mannose-coated nanofibers on bacterial agglutination and proliferation. The degree of agglutination is represented by the agglutination index (AI). Each value represents the mean  $\pm$  standard deviation (SD) of two independent experiments. (b) Growth curves based on the optical density (OD) at 600 nm for *E. coli* grown in the presence of **1**, **2**, and coassembled amphiphiles for 12 h. Each value represents the mean  $\pm$  SD of three independent experiments. (c) *E. coli* growth curves after addition of  $\alpha$ -methyl-D-mannopyranoside.

### Scheme 1. Schematic Representation of the Regulation of Agglutination and Proliferation of Bacterial Cells by Variation of the Nanofiber Length



that the length of the nanofibers would affect the size of the bacterial clusters and, subsequently, control bacteria proliferation. To confirm this hypothesis, we examined *E. coli* proliferation in the presence of mannose-coated nanofibers of different lengths. Spectrophotometric analysis based on turbidity or optical density (OD) is widely used to estimate the number of bacteria in liquid cultures.<sup>24,25</sup> As the population of bacterial cells grows, the intensity of transmitted light decreases. As the first step in proliferation experiments, an overnight culture of *E. coli* strain ORN 178 in Luria–Bertani (LB) medium was diluted in phosphate-buffered saline (PBS) until the OD at 600 nm (OD<sub>600</sub>) was 1.1–1.2. The *E. coli* suspension was mixed with aliquots of **1**, **2**, and coassembled samples in PBS. We measured the variation in the size of the *E. coli* population by measuring OD<sub>600</sub> every 30 min. As shown in Figure 6b, a normal bacterial growth curve was observed only in the presence of **2**. In contrast, we did not observe an increase in the cell population for **1** during our experimental time range. For the coassembled amphiphiles, the slope of the cell growth curve decreased with increasing **1** content. This result indicates that the proliferation of bacterial cells is regulated by the length of the carbohydrate-coated nanofibers, and this effect is attributed to the different agglutination forces for **1**, **2**, and the coassembled samples. This result indicates that the length of the nanofibers plays a critical role in regulating the proliferation of bacterial cells.

To determine whether this nanofiber is bacteriocidal or bacteriostatic, we added  $\alpha$ -methyl-D-mannopyranoside (Man) as a specific competitor in high excess (1000-fold) to an agglutinated solution containing amphiphile **1** that had been incubated for 4 h. After the addition of excess Man, the bacterial cells started to proliferate, demonstrating that the agglutination was reversible (Figure 6c).

In summary, we were able to control the fiber length of carbohydrate-coated nanofibers by the coassembly of carbohydrate-conjugated rod amphiphiles with different aromatic segments. The major driving force controlling the length of the fibers is the level of crystallinity of the fiber cores. The resulting carbohydrate-coated nanofibers with controlled lengths can systematically regulate biological functions, such as the agglutination and proliferation of specific bacterial cells.

## ■ ASSOCIATED CONTENT

### ● Supporting Information

Materials, methods, detailed experimental procedures (synthesis and cellular assays), compound characterization, and supporting figures. This material is available free of charge via the Internet at <http://pubs.acs.org>.

## ■ AUTHOR INFORMATION

### Corresponding Author

myongslee@snu.ac.kr

### Author Contributions

<sup>†</sup>D.-W.L. and T.K. contributed equally.

### Notes

The authors declare no competing financial interest.

## ■ ACKNOWLEDGMENTS

We thank Y.-b. Lim (Yonsei Univ.) for supplying *E. coli* strains ORN 178-GFP and ORN 208-RFP and for advice. We gratefully acknowledge the National Research Foundation of Korea (NRF) grant funded by the Korean Government

(MEST) (2012-0001240). We acknowledge a fellow of the BK21 Program of the Ministry of Education and Human Resource Development.

## ■ REFERENCES

- (1) Müller, M. K.; Brunsveld, L. *Angew. Chem., Int. Ed.* **2009**, *48*, 2921.
- (2) Lim, Y.; Park, S.; Lee, E.; Ryu, J. H.; Yoon, Y. R.; Kim, T. H.; Lee, M. *Chem.—Asian J.* **2007**, *2*, 1363.
- (3) Lim, Y.; Park, S.; Lee, E.; Jeong, H.; Ryu, J. H.; Lee, M. S.; Lee, M. *Biomacromolecules* **2007**, *8*, 1404.
- (4) Dolphin, G. T.; Dumy, P.; Garcia, J. *Angew. Chem., Int. Ed.* **2006**, *45*, 2699.
- (5) Baldwin, A. J.; Bader, R.; Christodoulou, J.; MacPhee, C. E.; Dobson, C. M.; Barker, P. D. *J. Am. Chem. Soc.* **2006**, *128*, 2162.
- (6) Hentschel, J.; Krause, E.; Börner, H. G. *J. Am. Chem. Soc.* **2006**, *128*, 7722.
- (7) Wang, H.; Gu, L.; Lin, Y.; Lu, F.; Meziani, M. J.; Luo, P. G.; Wang, W.; Cao, L.; Sun, Y. P. *J. Am. Chem. Soc.* **2006**, *128*, 13364.
- (8) Luo, P. G.; Wang, H.; Gu, L.; Lu, F.; Lin, Y.; Christensen, K. A.; Yang, S. T.; Sun, Y. P. *ACS Nano* **2009**, *3*, 3909.
- (9) Gregorio, C. C.; Weber, A.; Bondad, M.; Pennise, C. R.; Fowler, V. M. *Nature* **1995**, *377*, 83.
- (10) Gestwicki, J. E.; Christopher, W.; Strong, L. E.; Oetjen, K. A.; Kiessling, L. L. *J. Am. Chem. Soc.* **2002**, *124*, 14922.
- (11) Wang, X.; Guerin, G.; Wang, H.; Wang, Y.; Manners, I.; Winnik, M. A. *Science* **2007**, *317*, 644.
- (12) Guérin, G.; Wang, H.; Manners, I.; Winnik, M. A. *J. Am. Chem. Soc.* **2008**, *130*, 14763.
- (13) Gilroy, J. B.; Gädt, T.; Whittell, G. R.; Chabanne, L.; Mitchels, J. M.; Richardson, R. M.; Winnik, M. A.; Manners, I. *Nat. Chem.* **2010**, *2*, 566.
- (14) Besenius, P.; Portale, G.; Bomans, P. H. H.; Janssen, H. M.; Palmans, A. R. A.; Meijer, E. W. *Proc. Natl. Acad. Sci. U.S.A.* **2010**, *107*, 17888.
- (15) Bull, S. R.; Palmer, L. C.; Fry, N. J.; Greenfield, M. A.; Messmore, B. W.; Meade, T. J.; Stupp, S. I. *J. Am. Chem. Soc.* **2008**, *130*, 2742.
- (16) Moon, K.-S.; Kim, H.-J.; Lee, E.; Lee, M. *Angew. Chem., Int. Ed.* **2007**, *46*, 6807.
- (17) Lee, E.; Kim, J.-K.; Lee, M. *Angew. Chem., Int. Ed.* **2008**, *47*, 6375.
- (18) Huang, Z.; Lee, H.; Lee, E.; Kang, S.-K.; Nam, J.-M.; Lee, M. *Nat. Commun.* **2011**, *2*, 459.
- (19) Wolfenden, M. L.; Cloninger, M. J. *J. Am. Chem. Soc.* **2005**, *127*, 12168.
- (20) Mammen, M.; Choi, S.-K.; Whitesides, G. M. *Angew. Chem., Int. Ed.* **1998**, *37*, 2754.
- (21) Ryu, J.-H.; Lee, E.; Lim, Y.-b.; Lee, M. *J. Am. Chem. Soc.* **2007**, *129*, 4808.
- (22) Gestwicki, J. E.; Strong, L. E.; Cairo, C. W.; Boehm, F. J.; Kiessling, L. L. *Chem. Biol.* **2002**, *9*, 163.
- (23) Gu, L.; Elkin, T.; Jiang, X.; Li, H.; Lin, Y.; Qu, L.; Tzeng, T.-R. J.; Joseph, R.; Sun, Y.-P. *Chem. Commun.* **2005**, 874.
- (24) Wang, B.; Liu, P.; Jiang, W.; Pan, H.; Xu, X.; Tang, R. *Angew. Chem., Int. Ed.* **2008**, *47*, 3560.
- (25) Kim, J.; Ahn, Y.; Park, K. M.; Lee, D.-W.; Kim, K. *Chem.—Eur. J.* **2010**, *16*, 12168.